Published in final edited form as:
Anal Chem. 2012 November 6; 84(21): 9632–9639. doi:10.1021/ac3026064.

Genomic DNA extraction from cells by electroporation on an integrated microfluidic platform

Tao Geng[†], **Ning Bao**[‡,§], **Nammalwar Sriranganathanw**[‖], **Liwu Li**[⊥], and **Chang Lu**[*,‡,¶]

[†]Department of Agricultural and Biological Engineering, Purdue University, West Lafayette, IN 47907, USA

[‡]Department of Chemical Engineering, Virginia Tech, Blacksburg, VA 24061, USA

[§]School of Public Health, Nantong University, Nantong, Jiangsu, 226019, China

[‖]Department of Biomedical Sciences and Pathobiology, Virginia Tech, Blacksburg, VA 24061, USA

[⊥]Department of Biological Sciences, Virginia Tech, Blacksburg, VA 24061, USA

[¶]School of Biomedical Engineering and Sciences, Virginia Tech-Wake Forest University, Blacksburg, VA 24061, USA

Abstract

The vast majority of genetic analysis of cells involves chemical lysis for release of DNA molecules. However, chemical reagents required in the lysis interfere with downstream molecular biology and often require removal after the step. Electrical lysis based on irreversible electroporation is a promising technique to prepare samples for genetic analysis due to its purely physical nature, fast speed, and simple operation. However, there has been no experimental confirmation on whether electrical lysis extracts genomic DNA from cells in a reproducible and efficient fashion in comparison to chemical lysis, especially for eukaryotic cells that have most of DNA enclosed in the nucleus. In this work, we construct an integrated microfluidic chip that physically traps a low number of cells, lyses the cells using electrical pulses rapidly, then purifies and concentrates genomic DNA. We demonstrate that electrical lysis offers high efficiency for DNA extraction from both eukaryotic cells (up to ~36% for Chinese hamster ovary cells) and bacterial cells (up to ~45% for *Salmonella typhimurium*) that is comparable to the widely-used chemical lysis. The DNA extraction efficiency has dependence on both electric parameters and relative amount of beads used for DNA adsorption. We envision that electroporation-based DNA extraction will find use in ultrasensitive assays that benefit from minimal dilution and simple procedure.

INTRODUCTION

Microfluidics has revolutionized the way to conduct genomic studies and analyses in recent years.[1–8] Microfluidic devices offer dramatic reduction in the sample size and high level of automation which enable the analysis of genetic materials at the single molecule[9–13] and single cell level[14–18]. These devices typically integrate a number of steps ranging from cell lysis and DNA extraction/purification to PCR amplification. Successful DNA extraction that yields high purity and high abundance is the prerequisite for ultrasensitive detection and

[*]**Corresponding Author**: changlu@vt.edu. Phone: +1-540-231-8681. Fax: +1-540-231-5022.

Supporting Information
Additional information as noted in the text. This material is available free of charge via the Internet at http://pubs.acs.org.

analysis. Cells are typically lysed by disrupting the cell membrane for release of genetic materials. A variety of methods have been developed to lyse cells and microfluidic format accommodates most of these lysis methods.[19–21] Chemical lysis methods are most commonly used for DNA extraction either on-chip[22–27] or off-chip[28–34]. However, the lytic reagents including detergents, enzymes, chaotropic salts and alkaline may interfere with subsequent molecular assays. For example, the lytic reagent sodium dodecyl sulphate (SDS) significantly inhibits PCR amplification at a concentration as low as 0.01%.[35] Thus additional steps are typically required for the removal or dilution[17] of the lytic chemicals. These procedures add to the complexity of the device design and operation. More importantly, the associated material loss and dilution poses serious challenges for works requiring ultrahigh sensitivity (e.g. single cell studies at the whole genome level).

Electroporation has been an effective physical tool for breaching cell membrane barrier. In a typical electroporation process, a potential difference is built up across the cell membrane when a cell is exposed to an external electrical field. The induced transmembrane potential ($\Delta\psi_E$) is determined by $\Delta\psi_E = 1.5\, g(\lambda) rE \cos\theta$, where $g(\lambda)$ is a complex function of the membrane and buffer conductivities, r is the radius of the cell, E is the field intensity and θ is the angle between the normal to the membrane surface and the field direction.[36] When $\Delta\psi_E$ exceeds a threshold, the cell membrane can be irreversibly broken down, thus cell lysis and intracellular content release occur. Electroporation process is very rapid (on the order of milliseconds) and universally effective for bacterial and mammalian cells. Although electroporation has been successfully demonstrated for extraction of intracellular small molecules and proteins from both bacterial and eukaryotic cells[37–47], it remains unknown whether electroporation is effective for DNA extraction, especially in the case of eukaryotic cells with the genetic material enclosed by the nuclear envelope. There have been scarce reports related to DNA extraction by electroporation from bacterial cells.[48–50] However, there has been no similar demonstration on eukaryotic cells. Furthermore, our recent work suggested that the release of macromolecules such as proteins from eukaryotic cells were strongly affected by the molecule's subcellular location, with the nuclear localization being associated with more difficulty for release (compared to cytosolic localization).[51] Thus it is worth exploring whether extraction of genomic DNA (gDNA) from eukaryotic cells by electroporation is practical and under what conditions such extraction is efficient.

In this work, we combined electrical lysis with DNA purification on a microfluidic chip for preparing PCR-grade genomic DNA from both eukaryotic and bacterial cells. Chinese hamster ovary (CHO)-K1 cells and *Salmonella typhimurium* were electrically lysed, and the gDNA was purified using binding/desorption on ChargeSwitch beads and pressure-driven oscillatory washing before being quantified using real-time PCR off chip. We found that by applying high-intensity pulses (~2 kV/cm, a total duration of 1 s), electrical lysis yielded similar amount of gDNA from CHO-K1 cells as chemical lysis. This field intensity was substantially higher than the electroporation threshold (~400 V/cm) due to the difficulty associated with chromosomes escaping from the nuclear envelope. With similar electric parameters, we were able to produce more gDNA from *Salmonella* cells than chemical lysis. Our work suggests that electroporation yields similar or higher efficiency for extracting gDNA on a microfluidic platform for both eukaryotic and bacterial cells, compared to the popular chemical lysis approach. By eliminating chemicals, electroporation-based DNA extraction may significantly benefit ultrasensitive genetic analysis that requires simplicity in the operation and minimal dilution.

EXPERIMENTAL SECTION

Microfluidic chip design and fabrication

The polydimethylsiloxane (PDMS)/glass microfluidic chip, as shown in Figure 1, was constructed using multilayer soft lithography method[52, 53]. The two-layer microchip is composed of 55 μm deep control channels for pneumatic valve actuation on the top and 13 μm deep fluidic channels for sample transport and manipulation on the bottom. They are separated by a thin PDMS membrane. Some of the fluidic channels have rectangular cross section (250 μm wide) and thus can be partially closed when the microvalves are actuated, while the rest of the fluidic channels have a rounded cross section (300 μm wide) which are completely closed as the valves are engaged.

The microfabrication procedure was described previously with some modifications.[54, 55] Briefly, the two layers of channels were cast from two different master molds fabricated on 3-inch silicon wafers (University Wafer, South Boston, MA, USA). The control layer master was made of a negative photoresist SU-8 2025 (Microchem, Newton, MA, USA). The fluidic layer master was fabricated with a negative photoresist SU-8 2010 (Microchem) and a positive photoresist AZ 9260 (Clariant, Charlotte, NC, USA) to create the channels with rectangular and round cross sections, respectively. PDMS (GE Silicones, Wilton, CT, USA) prepolymer mixture consisting of monomer (RTV 615 A) and curing agent (RTV 615 B) at a mass ratio of 10:1.1 was poured onto the control layer master in a Petri dish to ~ 5 mm thick, and spun onto the fluidic layer master at 1100 rpm for 35 s to generate a thin membrane (~108 Mm thick). After partially curing both layers of PDMS at 80 °C for 30 min, the peeled control layer stamp was aligned and bonded to the fluidic layer by oxidization in a plasma cleaner (Harrick Plasma, Ithaca, NY, USA). The two-layer PDMS structure was then baked at 80 °C for another 30 min prior to being peeled off from the flow layer master and punched to generate access holes. To fabricate microelectrodes, an adhesion layer of titanium (20 nm thick; Kurt J. Lesker Company, Clairton, PA, USA) and a layer of gold (150 nm thick; Kurt J. Lesker Company) were sequentially deposited onto a pre-cleaned glass slide using an E-beam evaporator (PVD 250; Kurt J. Lesker Company). The pattern of electrodes was photolithographically defined on the slide by wet etching. The two-layer PDMS and the glass slide with microelectrodes were treated with oxygen plasma, aligned, and bonded together to form closed channels. Finally, the assembled chip was baked at 80 °C for another 2 h to ensure strong bonding between PDMS and the glass slide.

System setup and operation

The microfluidic chip was mounted on an inverted fluorescence microscope (IX-71; Olympus, Melville, NY, USA) equipped with 10× and 40× dry objectives and a CCD camera (ORCA-285; Hamamatsu, Bridgewater, NJ, USA). The reagents were introduced into the inlet via perfluoroalkoxyalkane (PFA) high purity tubing (IDEX Health & Science, Lake Forest, IL, USA) driven by a syringe pump (Fusion 400; Chemyx, Stafford, TX, USA). The actuation of both pneumatic valves and oscillatory washing was controlled by the application/removal of the pressure via solenoid valves (ASCO Scientific, Florham Park, NJ, USA) using a DAQ card (NI SCB-68; National Instruments, Austin, TX, USA) and a LabVIEW program (National Instruments). Electric voltages were provide by a DC power supply (PS350; Stanford Research Systems, Sunnyvale, CA, USA), and electrical pulses were generated by regulating the voltage through custom electronics including a high voltage reed relay (5501; Coto Technology, North Kingstown, RI, USA) using a LabVIEW program.

Cell preparation

CHO-K1 cells (ATCC, Manassas, VA, USA) were grown in F-12K medium (ATCC) supplemented with 10% fetal bovine serum (Invitrogen, Carlsbad, CA, USA) and 100 U/ml penicillin-100 mg/ml streptomycin (Invitrogen) at 37 °C in a humidified incubator containing 5% CO_2. Cells were subcultured every 2 days at a ratio of 1:10. Once harvested, the cells were washed and resuspended in electroporation buffer [8 mM Na_2HPO_4 (Sigma-Aldrich, St. Louis, MO, USA), 2 mM KH_2PO_4 (Sigma-Aldrich) and 250 mM sucrose (Sigma-Aldrich), pH 7.4] at a final concentration of 3×10^6 cells/ml. Cells were incubated on ice prior to use.

Salmonella typhimurium (ATCC) was grown in brain heart infusion (BHI; Sigma-Aldrich) broth in a shaking incubator at 37 °C for 5 h. The concentration (CFU/ml) was determined by plating 10-fold serial dilutions of bacterial cultures on BHI agar plates and counting colonies after overnight incubation at 37 °C. After collected by centrifugation at 4,000 *g* for 5 min at 4 °C, the bacterial cells were washed and resuspended in the electropoation buffer at desired concentrations. The cells were incubated on ice prior to use.

Fluorescent labeling of cells

CHO-K1 cells were fluorescently labelled by adding Hoechst 33342 (Invitrogen) stock solution (1 mg/ml) to cell suspension in culture medium (2×10^6 cells/ml) to a final concentration of 10 Mg/ml. After incubating the mixture at 37 °C for 45 min in the dark, the samples were centrifuged at 300 *g* for 5 min to remove excess dyes. The cell pellet was resuspended in the electroporation buffer before being introduced into the microchip.

Microfluidic cell lysis and DNA extraction

The analysis procedure performed on the microfluidic chip is illustrated in Figure 2. The microchannels were initially rinsed with the electroporation buffer containing 0.02% Tween 20 (Sigma-Aldrich) to reduce nonspecific adsorption of DNA to channel walls and expel bubbles. Subsequently, superparamagnetic ChargeSwitch beads (~1 Mm in diameter; Invitrogen) were loaded into the microchannels via the combined effects of pump-driven pressure and magnetic force generated by an external NdFeB permanent magnet (K&J Magnetics, Jamison, PA, USA) (Figure 2a). The partial closure of the valve allowed the liquid to pass through but retained the beads to form a packed bed (~ 1500 Mm long). For mammalian cells (CHO-K1), cell suspension flowed through the cell loading channel in order to introduce a certain number of cells and avoid the interference from cell stacking at the inlet port (Figure 2b). The cell number was determined by the volume of the loading channel (10 nl) and the concentration of the cell suspension, and in the meantime confirmed by visual inspection under the microscope. The cells were then efficiently trapped by the packed bed by infusing the electroporation buffer supplemented by 1 mg/ml of proteinase K (Sigma-Aldrich) into the channel (Figure 2c). For bacterial cells (*Salmonella typhimurium*), cells were directly introduced through the same inlet for bead loading. Proteinase K was added into the cell suspension with a final concentration of 1 mg/ml immediately prior to cell loading. Following the step, the DC power supply was connected to the surface electrodes to apply electrical pulses, during which all pneumatic valves were closed (Figure 2d). The cathode was put in the upstream of the packed bed. We typically applied 10 monopolar square electrical pulses with a frequency of 0.1 Hz and duration of 0.1 s for each pulse. While performing on-chip chemical lysis as a comparison, a small volume of Cell Lysis Solution (for mammalian cells; Qiagen, Valencia, CA, USA) or ChargeSwitch lysis buffer (for bacterial cells; Invitrogen) containing 1 mg/ml of proteinase K was introduced and incubated for 10 min. After cell lysis and gDNA release, ChargeSwitch binding buffer (Invitrogen) was introduced to selectively adsorb gDNA onto the beads (Figure 2e). The DNA-bound beads were then transferred into the large elliptical chamber and held by a

magnet, followed by washing with ChargeSwitch wash buffer (Invitrogen) to remove proteins and other contaminants (Figure 2f). In order to completely remove impurities, we applied 5 rounds of washing by oscillatory flow that moved the beads back and forth in the chamber (Figure 2g). In each round, the beads were exposed to oscillating pressure at a frequency of 20 Hz for 1.5 s. Afterwards, more contaminants were flushed out using wash buffer, during which a magnet was employed to immobilize the beads to a corner of the chamber (Figure 2h). All waste solutions flowed into outlet reservoir 1. Finally, the DNA-carrying beads were released into outlet reservoir 2 (Figure 2i), collected in a tube, and incubated in 20 Ml of 10 mM Tris-HCl buffer, pH 8.5 (Invitrogen) for 10 min to desorb gDNA.

Real-time PCR assay and data analysis

The amount of gDNA extracted was quantitatively measured by real-time PCR. All PCR assays were performed in 25 Ml reactions starting from 7.5 Ml of template DNA using iQ SYBR Green Supermix (Bio-Rad, Hercules, CA, USA) on an iQ5 thermocycler (Bio-Rad). Thermocycling conditions were 95 °C for 3 min followed by 40 cycles of 95 °C for 30 s and 60 °C for 30 s. The following primers (IDT, Coralville, IA, USA) were used to detect *GAPDH* gene in CHO-K1 cells and *Salmonella* invasion (*invA*) gene: *GAPDH* forward: 5'-TGGCAAAGTGGAAGTTGTTGCC-3' *GAPDH* reverse: 5'-TGCCTTTGAACTTGCCATGGGT-3' *invA* forward: 5'-TCGTCATTCCATTACCTACC-3' *invA* reverse: 5'-AAACGTTGAAAAACTGAGGA-3'

The absolute quantification of gDNA was carried out based on a PCR standard curve method. The standard curves were generated for each primer pairs and each PCR run based on 10-fold serial dilutions of a known amount of gDNA (measured by UV spectrophotometer at a wavelength of 260 nm). For each standard, the concentrations on a logarithmic scale were plotted against the PCR cycle threshold (Ct) values. The gDNA used for generating the standard curve was prepared using Generation Capture Column Kit (Qiagen) according to the manufacturer's instructions and dissolved in 10 mM Tris-HCl buffer, pH 8.5. The amounts of gDNA in unknown samples were calculated from their respective average PCR Ct values using the following formula:

$$[gDNA]=v\times 10^{\frac{(Ct-b)}{m}}$$

Where [gDNA] is the quantity of genomic DNA; v is the total volume of DNA sample; b and m are y intercept and slope of the standard curve, respectively. Every data point was presented based on the results of three independent on-chip experiments, and each experiment was conducted on a new microchip to avoid sample cross-contamination. All PCR reactions were run in duplicate.

RESULTS AND DISCUSSION

In this work, we designed a microfluidic chip for highly efficient extraction of gDNA from both mammalian and bacterial cell samples based on electroporation. Three distinct functional regions were integrated on a single microfluidic chip to reduce sample loss among various steps (Figure 1): (1) Cell and reagent loading. For processing bacterial cells, one inlet was used for infusing ChargeSwitch beads, various buffers and bacterial cell suspension. For CHO cell loading, a 10 nl segment of the microchannel with one inlet and one outlet was used for introducing a certain number of cells without accumulation at the entrance; (2) Electroporation. Cells were physically trapped by the packed ChargeSwitch beads and electrically lysed to release intracellular contents via applying pulses across the

planar gold electrodes. The gap between the two 100 Mm wide gold electrodes was 3 mm; (3) DNA purification. The dimensions of the elliptical chamber were 2 mm in the minor axis and 8 mm in the major axis, and the volume was approximately 110 nl. The bead-DNA complex was washed by pressure-driven oscillatory flow (There was an additional outlet for attaching to the pressure source). Elastomeric microvalves were used to either partially close (allowing liquid to pass through while blocking particles), or completely close (stopping the passage of both liquid and particles) the channel.[22] A permanent neodymium rare earth magnet was used to manipulate magnetic beads. As outlined in Figure 2, an entire on-chip analysis process was composed of constructing a packed bed of ChargeSwitch beads, loading cells, flushing cells against the beads and trapping cells, lysing cells with electrical pulses to release gDNA, adsorbing DNA onto beads, washing beads by pressure-driven oscillatory flow, and releasing DNA-bead complexes. The gDNA was finally recovered by incubating the DNA-carrying beads in high-pH buffer and then quantified by off-chip real-time PCR. It is worth noting that the change of the buffer between (d) electric lysis and (e) DNA binding does not lead to flushing of DNA out of the device because large genomic DNA can be physically trapped by the packed bed of beads (~1 Mm in diameter). DNA fragmentation should not happen under our conditions (it was reported that DNA fragmentation occurs under field intensity higher than 4.5 kV/cm[56]).

We chose ChargeSwitch magnetic beads for DNA extraction due to the mild conditions applied in the protocol. In each typical experiment, we utilized approximately 250 nl beads (diluted in 3 Ml solution when flowed into the device) having a potential binding capacity of 31.25 to 62.5 ng gDNA (according to the manual of ChargeSwitch kit). The beads were packed in the microchannel to form a matrix-like structure for physical trapping of either CHO-K1 or *Salmonella* cells between the two electrodes. The trapping efficiency was nearly 100%, as evidenced in our previous publications[44, 54].

Washing is a critical step in DNA solid-phase extraction to remove potential PCR inhibitors. We devised a pressure-driven washing procedure to efficiently mix the beads and washing buffer and remove intracellular molecules other than DNA from the bead surface (shown in Fig. 2g and SI Figure S1). The fluidic chamber was connected to the pressure source (a nitrogen cylinder) via solenoid valves. The application and removal of the pressure was automatically oscillated by switching on/off the solenoid valves via a LabVIEW program. Beads were pushed forwards and backwards in washing buffer during the process. The range of bead movement inside the chamber could be adjusted by changing the applied pressure and the oscillatory frequency. The wash process was very fast (~1.5 s) and worked similarly to pipetting up and down in a centrifuge tube. As shown in SI Figure S1b, the beads could be dispersed loosely in the microchannel, which greatly increased the contact area of beads with the wash buffer.

Square DC electrical pulses were used to perform electroporation, as the highest transmembrane potential would be imposed on the cell membrane under this condition. The gold electrodes were integrated into the microchip and directly in contact with the fluid in the chamber, thus gases (hydrogen and oxygen) would be inevitably produced on the electrode surface when an applied voltage exceeded the threshold for water electrolysis. The accumulation of gases in the microfluidic chamber would form bubbles and affect the manipulation of the fluid. We found that conducting the electroporation in a closed chamber facilitated the permeabilization of gases through PDMS walls and alleviated issues associated with bubbles. Figure 3 shows the time-lapse images of bubbles generate in the vicinity of the cathode when an electric field intensity of 2.2 kV/cm was applied for 0.1 s. When the pneumatic valves at the chamber inlet and outlet were closed (Fig. 3a), the gas bubbles generated were relatively small and they gradually disappeared over time (in a period of 10 s) due to permeabilization through PDMS. In contrast, if the pneumatic valves

were open (Fig. 3b), the large bubbles filled in the channel and there was no substantial decrease in the bubble size after 10 s.

In order to visualize DNA extraction from mammalian cells, we fluorescently labelled CHO-K1 cells with Hoechst 33342 that stain nuclei of living cells and loaded 75 labelled cells into the chamber. A serial of DC square pulses with a total duration of 1 s (10 pulses each of 2.2 kV/cm, 0.1 s duration with 9.9 s interval in between) were applied. Figure 4 shows the change in the cell morphology (examined by DIC microscopy) and the fluorescence during the application of the pulses. Prior to exposure to electrical pulses, the cells having intact membranes were stacked against the packed beads (Figure 4a and 4e). After the application of the first electrical pulse, the shape of the cells became less well-defined (Figure 4b) and there was decrease in the fluorescence intensity of cells due to release of gDNA (Figure 4f). These suggest the onset of electroporation. The released labelled gDNA was not obvious in the images, presumably due to rapid dilution and movement in the electric field. Figure 4c and 4g show that after five pulses, the cells became amorphous mass and there was dramatic decrease in the fluorescence intensity. Finally there was very little fluorescence left in the cells after 10 pulses (Figure 4d and 4h). The results indicate the applied electroporation conditions were sufficient for high efficiency gDNA release.

By using 10 pulses of 0.1 s each and 9.9 s intervals in between, we varied the field intensity in the range from 0 to 2.2 kV/cm to evaluate its influence on gDNA release from CHO-K1 cells. We loaded ~30 CHO-K1 cells in the chamber and quantified the amount of *GAPDH* gene resulted from the DNA extraction by real-time PCR. The PCR Ct values of *GAPDH* gene were converted into the quantity of genomic DNA by comparing with the PCR standard curves derived from the serial dilutions of CHO-K1 cell total gDNA whose concentration was measured by UV spectroscopy. The gDNA yield was further normalized to the amount of gDNA generated per cell. As expected, higher electric field intensities yielded more gDNA release, as shown in Figure 5. In the best case, we were able to achieve the maximal yield of 1.8 ± 0.2 pg DNA/cell at the field intensity of 2.2 kV/cm. Based on the reported CHO-K1 genome size of 2.6×10^9 bp[57] (equivalent to ~5 pg DNA/cell) and the hypodiploid nature of CHO-K1 cells, the extraction efficiency was estimated to be at least ~36 ± 4%. A negative control assay where no voltage was applied exhibited little yield (0.03 ± 0.02 pg DNA/cell), suggesting that electroporation was the main mechanism for DNA release. As a benchmark, we also conducted on-chip chemical lysis for DNA extraction using a commercial chemical lysis buffer. The yield by chemical lysis (1.9 ± 0.1 pg DNA/cell) was very similar to the best result by electroporation.

We also extracted gDNA from gram-negative bacterium *Salmonella typhimurium* using similar electroporation parameters and quantified the amount by examining *Salmonella* specific *invA* gene. Since the genome of *Salmonella typhimurium* (haploid cells) is approximately 4.8×10^6 bp[58] with corresponding DNA quantity of ~0.005 pg/cell, we used 10^4 CFU of bacterial cells in the microfluidic chamber for processing in each trial. Figure 6a shows that exposure of cells to higher field intensity was generally preferable for effective cell lysis and DNA release. The highest yield was 10.8 ± 2.1 pg DNA from 10^4 cells (with an extraction efficiency of ~22 ± 4%) when they were treated at the field intensity of 2.0 kV/cm. Electrical lysis could produce more gDNA at high field intensities (≥1.8 kV/cm) than chemical lysis (7.6 ± 2.3 pg DNA). This is attributed to the fact that no heating was involved in our on-chip chemical lysis procedure, possibly leading to inefficient cell disruption in lysis buffer for bacterial cells (Typically, heating at 80 °C for 1 to 1.5 h would be ideal to completely disintegrate the rigid bacterial cell walls). It is worth noting that on our microfluidic platform, the final DNA extraction efficiency was also affected by the amount of ChargeSwitch beads used for DNA adsorption and such bead amount needs to be optimized for a given number of cells. In Figure 6b, the number of *Salmonella* cells was

varied from 10^2 to 10^6 CFU, and 10 pulses of 0.1 s and 1.8 kV/cm and 250 nl beads were applied in all cases for the assay. The results reveal that the extraction efficiency increased from 5 ± 0.6% to 45 ± 10% while varying the CFU of bacterial cells from 10^6 to 10^2. This suggests that increased bead surface area/cell number ratio promotes higher extraction efficiency. The amount of beads we used (250 nl) appears to be ideal for processing 10^2-10^3 *Salmanella* cells under the conditions.

Even without optimized bead amount for each cell number, the performance of our microfluidic assays was still quite comparable to that of commercial Qiagen Generation Capture column kit (SI Figure S2). We also found that the addition of proteinase K improved DNA extraction in our process (SI Figure S3). This is possibly because the protease efficiently digested the histone proteins and other DNA-binding nuclear components, which facilitated the liberation of DNA from the nuclei. In addition, the enzyme could inactivate the nucleases naturally existing in cells and thus prevent DNA molecules from being degraded.

It is interesting to note that although bacterial cells generally have much higher electroporation threshold than mammalian cells (e.g. 1000–1500 V/cm for onset of electroporation for *E. coli*[42] vs. 300–400 V/cm for CHO-K1 cells[59, 60] due to their smaller sizes and different membrane properties, the required field intensity for successful DNA extraction is similar for *Salmanella* and CHO-K1 cells as revealed above. This is presumably because of the difficulty of releasing chromosomes from nucleus in the case of eukaryotic cells. Electrochemical lysis (i.e. lysis due to the generation of hydroxide ions at cathode by electrolysis)[61, 62] was not likely to be important in our process. We kept the distance between two electrodes at 3 mm and trapped cells in the middle (approximately 1.5 mm away from the cathode) where the buffer was generally neutral.

Supplementary Material

Refer to Web version on PubMed Central for supplementary material.

Acknowledgments

This work was supported by United States Department of Agriculture [NRI 2009-35603-05059 to C.L.], National Science Foundation [CBET 1016547, 0967069 to C.L.], ICTAS NanoBio Thrust grant [to C.L.] and National Institutes of Health [HL115835 to L.L.].

REFERENCES

1. Pal R, Yang M, Lin R, Johnson BN, Srivastava N, Razzacki SZ, Chomistek KJ, Heldsinger DC, Haque RM, Ugaz VM, Thwar PK, Chen Z, Alfano K, Yim MB, Krishnan M, Fuller AO, Larson RG, Burke DT, Burns MA. Lab Chip. 2005; 5:1024–1032. [PubMed: 16175256]
2. Yager P, Edwards T, Fu E, Helton K, Nelson K, Tam MR, Weigl BH. Nature. 2006; 442:412–418. [PubMed: 16871209]
3. Zhang C, Xing D. Nucleic Acids Res. 2007; 35:4223–4237. [PubMed: 17576684]
4. Chen L, Manz A, Day PJ. Lab Chip. 2007; 7:1413–1423. [PubMed: 17960265]
5. Agrawal N, Hassan YA, Ugaz VM. Angew. Chem. Int. Edit. 2007; 46:4316–4319.
6. Liu P, Mathies RA. Trends Biotechnol. 2009; 27:572–581. [PubMed: 19709772]
7. Price CW, Leslie DC, Landers JP. Lab Chip. 2009; 9:2484–2494. [PubMed: 19680574]
8. McCalla SE, Tripathi A. Annu. Rev. Biomed. Eng. 2011; 13:321–343. [PubMed: 21568712]
9. Yeh HC, Chao SY, Ho YP, Wang TH. Curr. Pharm. Biotechnol. 2005; 6:453–461. [PubMed: 16375730]
10. Brewer LR, Bianco PR. Nat. Methods. 2008; 5:517–525. [PubMed: 18511919]

11. Zhang C, Xing D. Chem. Rev. 2010; 110:4910–4947. [PubMed: 20394378]
12. Heyries KA, Tropini C, VanInsberghe M, Doolin C, Petriv OI, Singhal A, Leung K, Hughesman CB, Hansen CL. Nat. Methods. 2011; 8:649–651. [PubMed: 21725299]
13. Men Y, Fu Y, Chen Z, Sims PA, Greenleaf WJ, Huang Y. Anal. Chem. 2012; 84:4262–4266. [PubMed: 22482776]
14. Ottesen EA, Hong JW, Quake SR, Leadbetter JR. Science. 2006; 314:1464–1467. [PubMed: 17138901]
15. Kalisky T, Blainey P, Quake SR. Annu. Rev. Genet . 2011; 45:431–445. [PubMed: 21942365]
16. Lecault V, Vaninsberghe M, Sekulovic S, Knapp DJ, Wohrer S, Bowden W, Viel F, McLaughlin T, Jarandehei A, Miller M, Falconnet D, White AK, Kent DG, Copley MR, Taghipour F, Eaves CJ, Humphries RK, Piret JM, Hansen CL. Nat. Methods. 2011; 8:581–586. [PubMed: 21602799]
17. White AK, VanInsberghe M, Petriv OI, Hamidi M, Sikorski D, Marra MA, Piret J, Aparicio S, Hansen CL. Proc. Natl. Acad. Sci. U.S.A. 2011; 108:13999–14004. [PubMed: 21808033]
18. Fan HC, Wang JB, Potanina A, Quake SR. Nat. Biotechnol. 2011; 29:51–57. [PubMed: 21170043]
19. Kim J, Johnson M, Hill P, Gale BK. Integr. Biol. 2009; 1:574–586.
20. He MY, Edgar JS, Jeffries GDM, Lorenz RM, Shelby JP, Chiu DT. Anal. Chem. 2005; 77:1539–1544. [PubMed: 15762555]
21. Jeffries GDM, Edgar JS, Zhao YQ, Shelby JP, Fong C, Chiu DT. Nano Lett. 2007; 7:415–420. [PubMed: 17298009]
22. Hong JW, Studer V, Hang G, Anderson WF, Quake SR. Nat. Biotechnol. 2004; 22:435–439. [PubMed: 15024389]
23. Marcus JS, Anderson WF, Quake SR. Anal.Chem. 2006; 78:3084–3089. [PubMed: 16642997]
24. Easley CJ, Karlinsey JM, Bienvenue JM, Legendre LA, Roper MG, Feldman SH, Hughes MA, Hewlett EL, Merkel TJ, Ferrance JP, Landers JP. Proc. Natl. Acad. Sci. U.S.A. 2006; 103:19272–19277. [PubMed: 17159153]
25. Bienvenue JM, Duncalf N, Marchiarullo D, Ferrance JP, Landers JP. J. Forensic Sci. 2006; 51:266–273. [PubMed: 16566759]
26. Chen X, Cui da F, Liu CC. Electrophoresis. 2008; 29:1844–1851. [PubMed: 18393339]
27. Mahalanabis M, Al-Muayad H, Kulinski MD, Altman D, Klapperich CM. Lab Chip. 2009; 9:2811–2817. [PubMed: 19967118]
28. Cady NC, Stelick S, Batt CA. Biosens. Bioelectron. 2003; 19:59–66. [PubMed: 14558999]
29. Chung YC, Jan MS, Lin YC, Lin JH, Cheng WC, Fan CY. Lab Chip. 2004; 4:141–147. [PubMed: 15052355]
30. Legendre LA, Bienvenue JM, Roper MG, Ferrance JP, Landers JP. Anal. Chem. 2006; 78:1444–1451. [PubMed: 16503592]
31. Cao W, Easley CJ, Ferrance JP, Landers JP. Anal.Chem. 2006; 78:7222–7228. [PubMed: 17037925]
32. Kim J, Gale BK. Lab Chip. 2008; 8:1516–1523. [PubMed: 18818807]
33. Persat A, Marshall LA, Santiago JG. Anal. Chem. 2009; 81:9507–9511. [PubMed: 19831356]
34. Karle M, Miwa J, Czilwik G, Auwarter V, Roth G, Zengerle R, von Stetten F. Lab Chip. 2010; 10:3284–3290. [PubMed: 20938545]
35. Goldenberger D, Perschil I, Ritzler M, Altwegg M. PCR Methods Appl. 1995; 4:368–370. [PubMed: 7580932]
36. Weaver JC, Chizmadzhev YA. Bioelectrochem. Bioener. 1996; 41:135–160.
37. McClain MA, Culbertson CT, Jacobson SC, Allbritton NL, Sims CE, Ramsey JM. Anal. Chem. 2003; 75:5646–5655. [PubMed: 14588001]
38. Han F, Wang Y, Sims CE, Bachman M, Chang R, Li GP, Allbritton NL. Anal. Chem. 2003; 75:3688–3696. [PubMed: 14572031]
39. Gao J, Yin XF, Fang ZL. Lab Chip. 2004; 4:47–52. [PubMed: 15007440]
40. Munce NR, Li J, Herman PR, Lilge L. Anal. Chem. 2004; 76:4983–4989. [PubMed: 15373432]
41. Lu H, Schmidt MA, Jensen KF. Lab Chip. 2005; 5:23–29. [PubMed: 15616736]
42. Wang HY, Bhunia AK, Lu C. Biosens. Bioelectron. 2006; 22:582–588. [PubMed: 16530400]

43. Wang HY, Lu C. Chem. Commun. 2006:3528–3530.
44. Bao N, Lu C. Appl. Phys. Lett. 2008; 92:214103.
45. Nakayama T, Namura M, Tabata KV, Noji H, Yokokawa R. Lab Chip. 2009; 9:3567–3573. [PubMed: 20024037]
46. Boukany PE, Morss A, Liao WC, Henslee B, Jung HC, Zhang XL, Yu B, Wang XM, Wu Y, Li L, Gao KL, Hu X, Zhao X, Hemminger O, Lu W, Lafyatis GP, Lee LJ. Nat. Nanotechnol. 2011; 6:747–754. [PubMed: 22002097]
47. Henslee BE, Morss A, Hu X, Lafyatis GP, Lee LJ. Anal. Chem. 2011; 83:3998–4003. [PubMed: 21473595]
48. Cheng J, Sheldon EL, Wu L, Uribe A, Gerrue LO, Carrino J, Heller MJ, O'Connell JP. Nat. Biotechnol. 1998; 16:541–546. [PubMed: 9624684]
49. Vitzthum F, Geiger G, Bisswanger H, Elkine B, Brunner H, Bernhagen J. Nucleic Acids Res. 2000; 28:e37. [PubMed: 10734214]
50. Vulto P, Dame G, Maier U, Makohliso S, Podszun S, Zahn P, Urban GA. Lab Chip. 2010; 10:610–616. [PubMed: 20162236]
51. Zhan YH, Martin VA, Geahlen RL, Lu C. Lab Chip. 2010; 10:2046–2048. [PubMed: 20548993]
52. Unger MA, Chou HP, Thorsen T, Scherer A, Quake SR. Science. 2000; 288:113–116. [PubMed: 10753110]
53. Thorsen T, Maerkl SJ, Quake SR. Science. 2002; 298:580–584. [PubMed: 12351675]
54. Geng T, Bao N, Litt MD, Glaros TG, Li L, Lu C. Lab Chip. 2011; 11:2842–2848. [PubMed: 21750827]
55. Awwad Y, Geng T, Baldwin AS, Lu C. Anal. Chem. 2012; 84:1224–1228. [PubMed: 22263650]
56. Hofmann F, Ohnimus H, Scheller C, Strupp W, Zimmermann U, Jassoy C. J. Membrane Biol. 1999; 169:103–109. [PubMed: 10341032]
57. Xu X, Nagarajan H, Lewis NE, Pan SK, Cai ZM, Liu X, Chen WB, Xie M, Wang WL, Hammond S, Andersen MR, Neff N, Passarelli B, Koh W, Fan HC, Wang JB, Gui YT, Lee KH, Betenbaugh MJ, Quake SR, Famili I, Palsson BO, Wang J. Nat. Biotechnol. 2011; 29:735–741. [PubMed: 21804562]
58. McClelland M, Sanderson KE, Spieth J, Clifton SW, Latreille P, Courtney L, Porwollik S, Ali J, Dante M, Du F, Hou S, Layman D, Leonard S, Nguyen C, Scott K, Holmes A, Grewal N, Mulvaney E, Ryan E, Sun H, Florea L, Miller W, Stoneking T, Nhan M, Waterston R, Wilson RK. Nature. 2001; 413:852–856. [PubMed: 11677609]
59. Wang HY, Lu C. Anal.Chem. 2006; 78:5158–5164. [PubMed: 16841942]
60. Wang HY, Lu C. Biotechnol. Bioeng. 2006; 95:1116–1125. [PubMed: 16817188]
61. Di Carlo D, Ionescu-Zanetti C, Zhang Y, Hung P, Lee LP. Lab Chip. 2005; 5:171–178. [PubMed: 15672131]
62. Lee HJ, Kim JH, Lim HK, Cho EC, Huh N, Ko C, Park JC, Choi JW, Lee SS. Lab Chip. 2010; 10:626–633. [PubMed: 20162238]

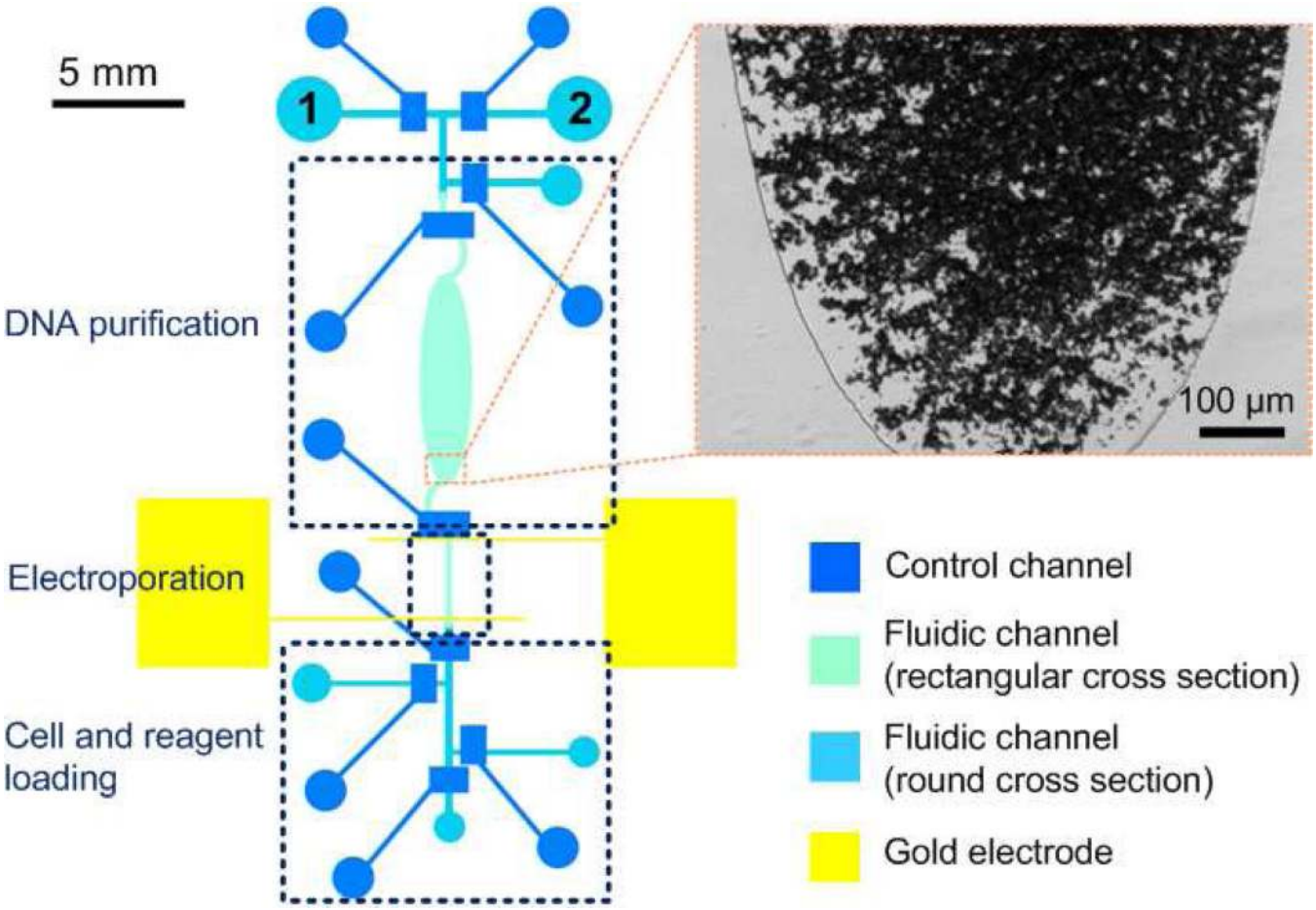

Figure 1.

Design of an integrated microfluidic chip for electrical lysis and DNA extraction. The microfluidic chip consists of a control layer for pneumatic valve actuation (blue) and a fluidic layer for sample transport and manipulation (light green and light blue). Once the valves are actuated, the fluidic channel having a rectangular cross section (light green) is partially closed, and the one with a round cross section (light blue) is fully closed. Gold (yellow) is deposited on glass surface to sever as electrodes. The chip contains three regions: (1) cell and reagent loading region; (2) electroporation region for bead/cell capture and electrical lysis; and (3) an elliptical chamber for DNA purification. There are two outlet reservoirs for collecting waste (labelled “1”) and DNA-carrying magnetic beads (labeled “2”). The inset image illustrates magnetic beads dispersed in the elliptical chamber.

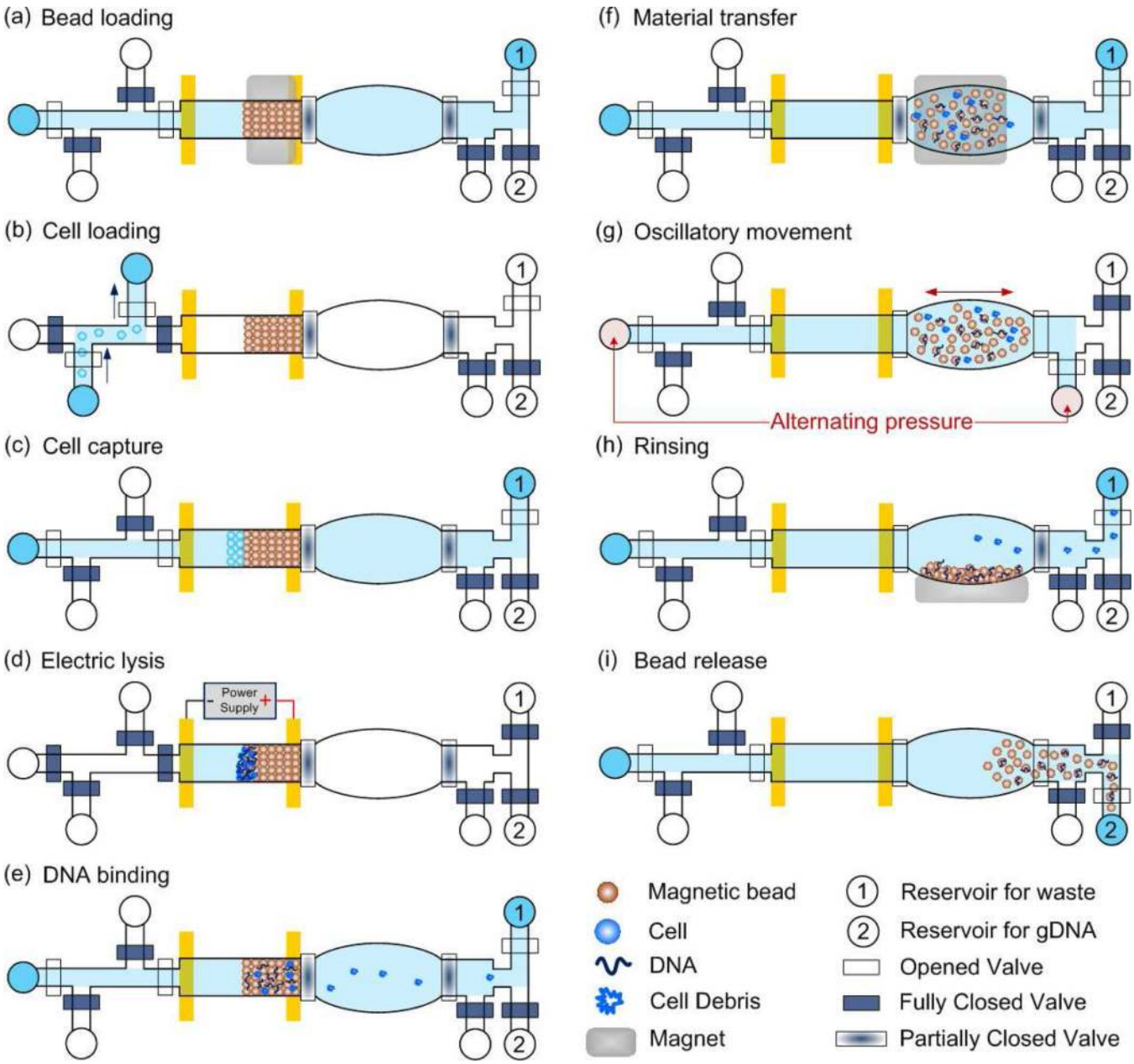

Figure 2.

Schematic diagram of on-chip procedure for microfluidic electrical lysis and DNA extraction. (a) Magnetic beads are loaded into the microchannel and blocked by a partially closed valve to form a packed bed; (b) Mammalian cells are flowed into the loading channel and a certain number of cells are confined in the channel; (c) Electroporation buffer is infused to push cells against the bead bed and makes them physically trapped; (d) Cells are electrically lysed; (e) gDNA is selectively bound onto beads in low-pH buffer; (f) Beads are transferred into the elliptical chamber, held by a magnet, and washed with aqueous buffer to remove contaminants; (g) Beads are moved back and forth in oscillatory flow driven by alternating pressure; (h) Residual contaminants are eliminated by one more rinsing step; and (i) DNA-carrying beads are released into an outlet reservoir.

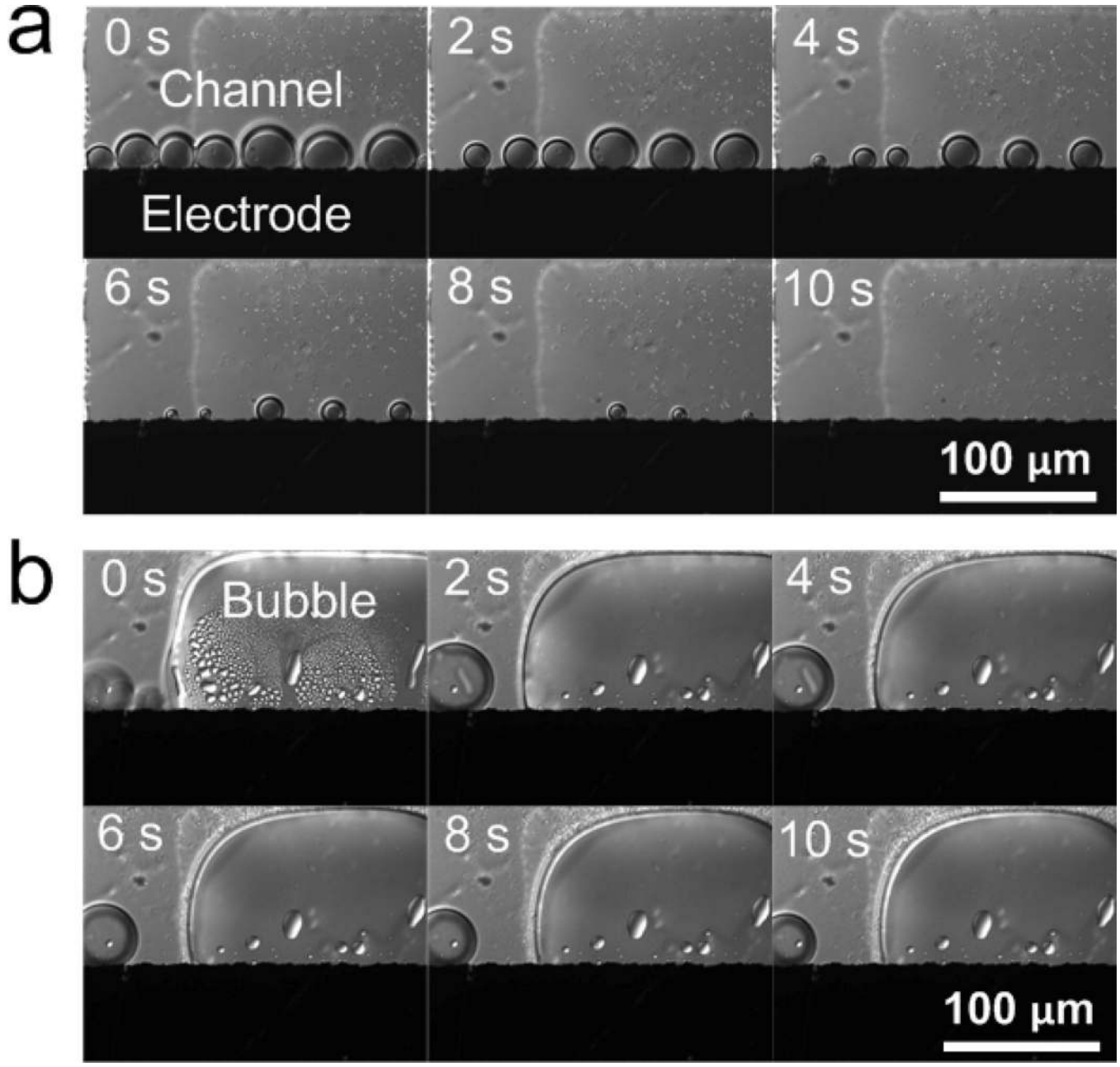

Figure 3.

Time-lapse imaging of bubble generation in the vicinity of the cathode. The bubbles were generated by applying an electrical pulse with a duration of 0.1 s and a field intensity of 2.2 kV/cm at t=0 s. (a) When all microvalves were closed, the bubbles were relatively small, and gradually disappeared in 10 s. (b) When all microvalves were open, the bubbles were large, and exhibited almost no change in 10 s.

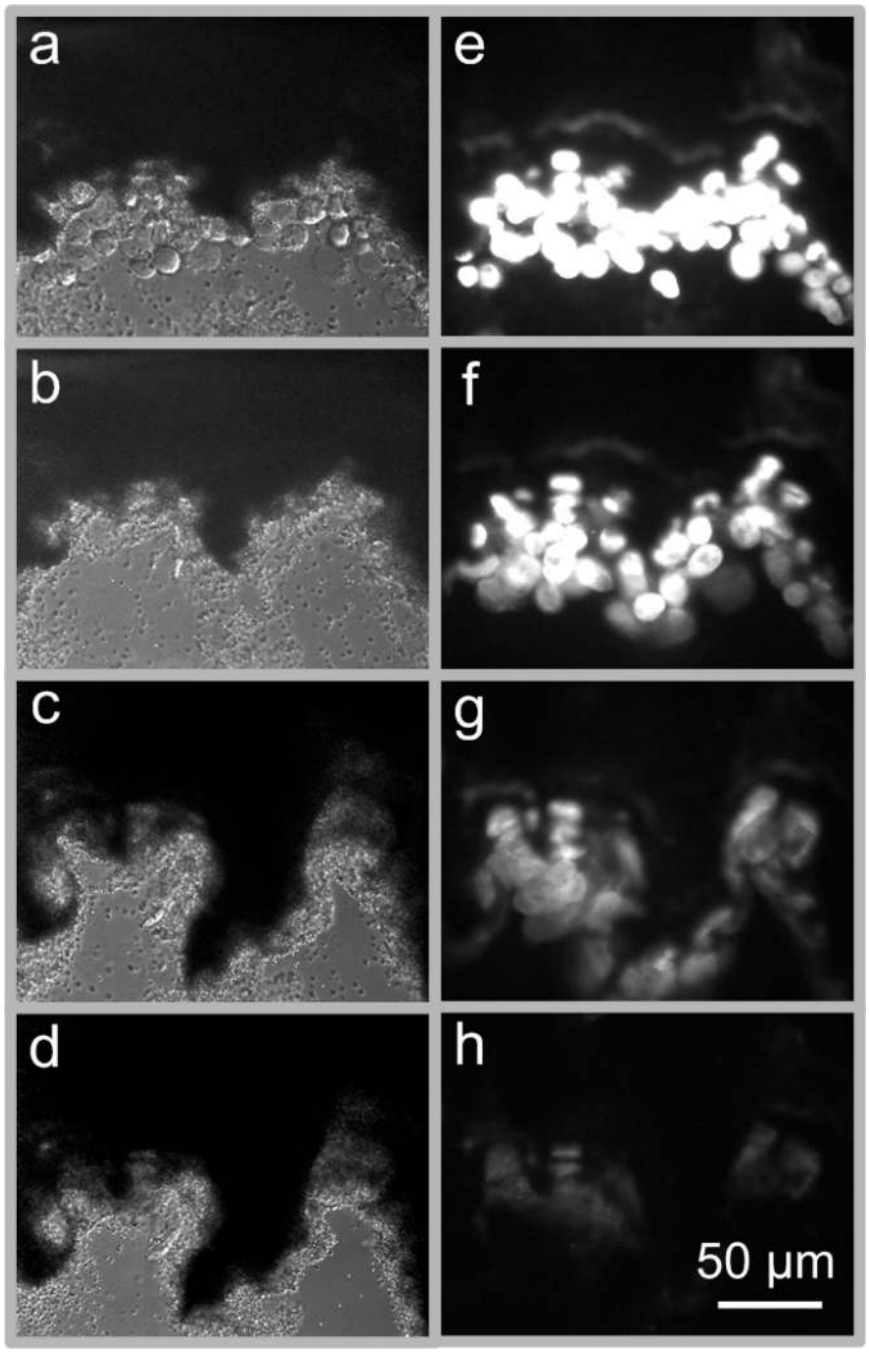

Figure 4.

Differential interference contrast (DIC) images (a-d) and corresponding fluorescence images (e-h) of CHO-K1 cells before electrical lysis (a and e) and after the treatment of 1 (b and f), 5 (c and g) and 10 (d and h) electrical pulses. 75 cells were fluorescently labelled with Hoechst 33342, physically trapped by the bead bed, and then exposed to square DC electrical pulses (0.1 s duration for each pulse with 9.9 s in between) with a field intensity of 2.2 kV/cm. The reducing fluorescent intensity and the morphological changes of cells indicate that cells are efficiently lysed and DNA molecules are released out of the cells.

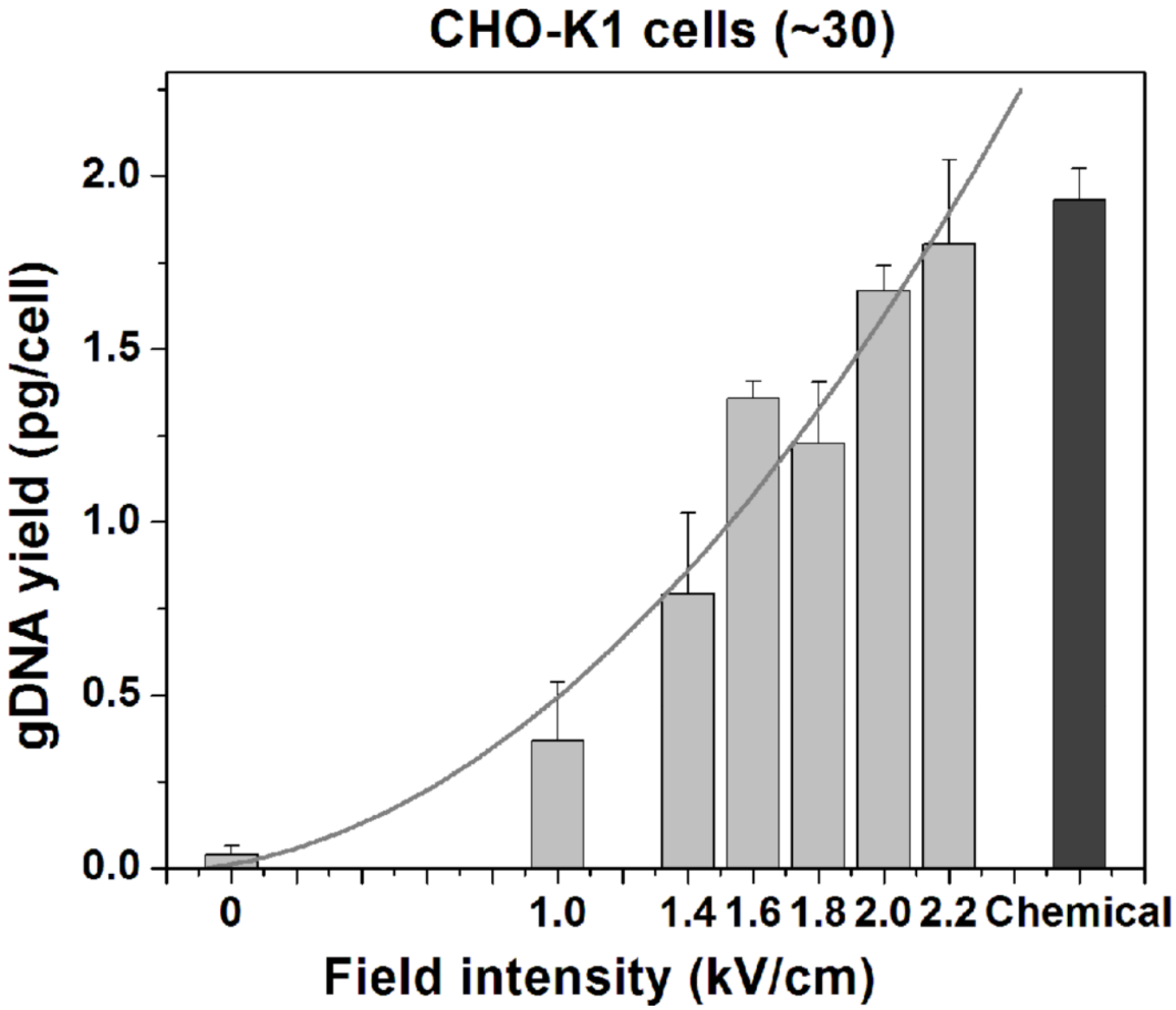

Figure 5.
DNA extraction from CHO-K1 cells. Approximately 30 cells were electrically lysed by 10 square DC electrical pulses (0.1 s duration for each pulse with 9.9 s in between) at various field intensities (grey bars) or chemically lysed by Qiagen lysis buffer (black bar). *GAPDH* gene was targeted. gDNA yield was quantified by real-time PCR, and normalized against the cell number.

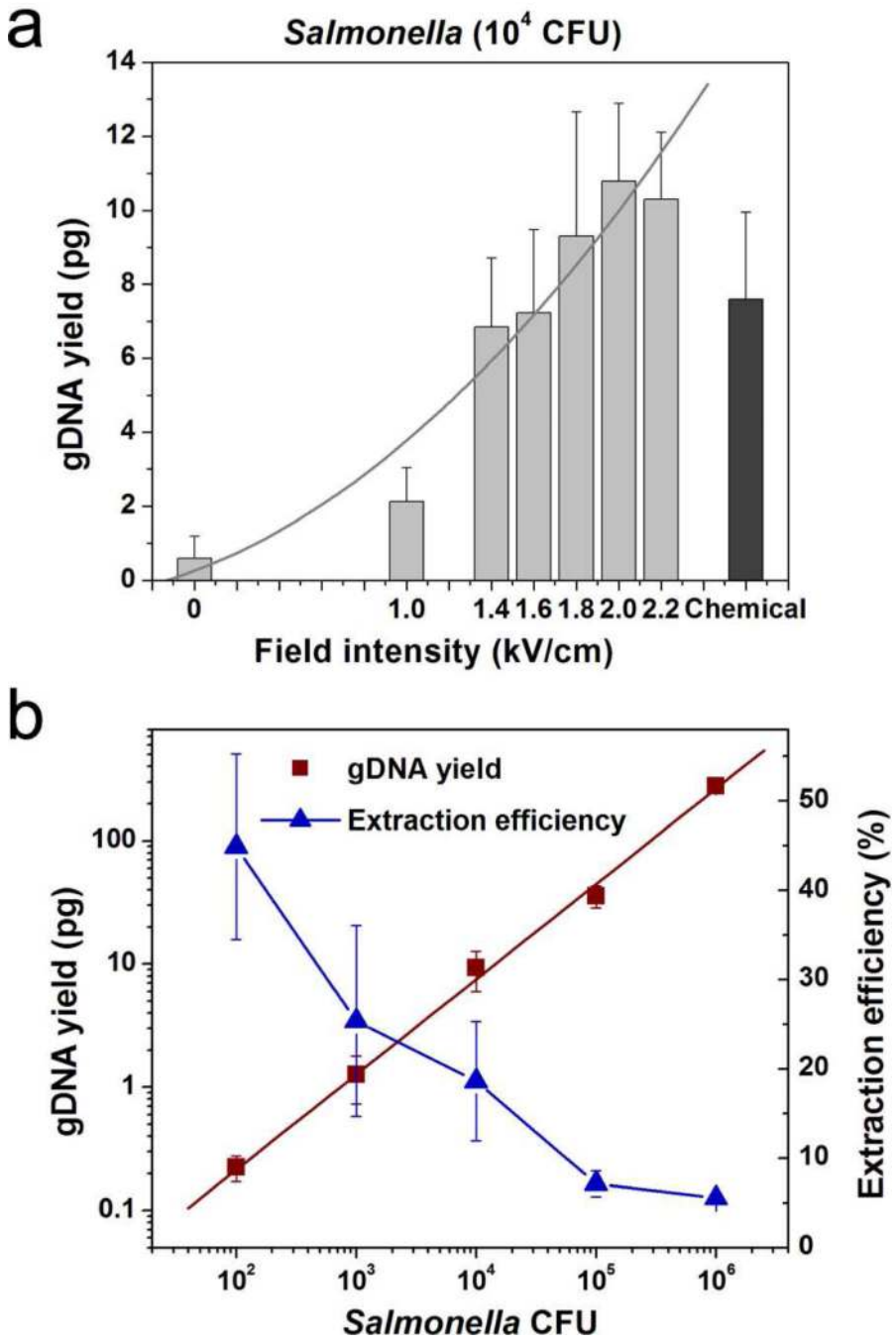

Figure 6.

DNA extraction from *Salmonella*. (a) 10^4 CFU of the bacterial cells were electrically lysed at varying field intensities (grey bars) or chemically lysed by ChargeSwitch lysis buffer (black bar). (b) Bacterial samples with varying initial CFU (10^2 to 10^6) were electrically lysed at a field intensity of 1.8 kV/cm. For all electrical lysis experiments, 10 square DC electrical pulses (0.1 s duration for each pulse with 9.9 s in between) were applied. *Salmonella* specific *invA* gene was targeted, and gDNA yield was quantified by real-time PCR. The extraction efficiency is calculated by dividing gDNA yield by total gDNA amount (assuming the genome of *Salmonella typhimurium* is ~0.005 pg/cell).